J Math Chem (2015) 53:1412–1425
DOI 10.1007/s10910-015-0496-4

ORIGINAL PAPER

Dynamic hysteresis in the velocity and dissipation of stochastic Michaelis–Menten kinetics

Kinshuk Banerjee[1]

Received: 17 January 2015 / Accepted: 23 March 2015 / Published online: 28 March 2015

Abstract In this work, we have studied a single molecule enzyme catalysis reaction in presence of oscillatory substrate concentration. The stochastic kinetics is modelled in terms of a chemical master equation. Depending on the oscillation frequency, hysteresis can occur in the system which is dynamic in nature. The time-dependent driving keeps the system out-of-equilibrium associated with dissipation. The interplay between the timescales of the system kinetics and the external driving necessitates the splitting of the total entropy production rate into adiabatic and nonadiabatic contributions. Analyses of these quantities give insights into the various balance conditions of the reaction fluxes and their roles in governing the nonequilibrium thermodynamics of the system. Interestingly, the net velocity of catalysis and the dissipation along with its various parts are found to exhibit hysteresis that vanish in the low and high-frequency ranges of substrate oscillation. However, the average (over a period) velocity as well as the average dissipation show hyperbolic increase with frequency to saturation. We have proposed an experimental protocol to realize such features using periodic stepwise injection of substrate at specified rates.

Keywords Stochastic enzyme kinetics · Dissipation · Dynamic hysteresis

1 Introduction

Advent of single molecule spectroscopic techniques has revolutionized the field of chemical kinetics by revealing the details, at least, at the mesoscopic scale [1–7]. Progress in this direction not only added a new dimension to the experimental field

✉ Kinshuk Banerjee
banerjee.kinshuk8@gmail.com

[1] Department of Chemistry, University of Calcutta, Kolkata 700009, India

[8] but also rekindled interest in the theoretical treatment [9–11]. The latter primarily involves the stochastic theory of chemical reactions [12,13]. This is mainly based on the chemical master equation (CME) [14,15] where the concentrations are replaced by the corresponding probabilities of population states [16]. The approach has been developed over the years [17,18], with its significance now growing rapidly as experimental realizations come into light. Comparison of the bulk kinetics, governed by deterministic rate equations, with the stochastic occurrence of reaction events, described by the CME, provides valuable insights into the special features of reactions of small systems and inside tiny volumes, e.g., inside a living cell [19,20]. In this context, enzyme catalysis remains an attractive choice as a reaction system having tremendous biological importance [21]. The seminal Michaelis–Menten (MM) reaction scheme [22] still holds a key place as the reference frame for all the theories going beyond its limitations. The validity of the MM kinetics in the stochastic domain has been tested in terms of the variables of single molecule experiments that also furnish data giving deeper knowledge of reaction mechanism [23].

The stochastic approach is not only applied to kinetics but also to the corresponding thermodynamics [24–27]. Construction of nonequilibrium thermodynamics in terms of master equation as a self-consistent theory is an active area of research [28–31]. The link with reaction systems comes in the form of nonequilibrium steady state (NESS) [32], attained by the system in presence of sustained driving [33]. In a NESS, detailed balance is broken (satisfied in equilibrium) and a positive dissipation exists (vanishes in equilibrium), although the concentrations (or probabilities) become fixed in time [34]. In the case of MM kinetics, such a NESS can be achieved by assuming the chemiostatic condition where the substrate and product concentrations are kept constant by suitable inflow and outflow, respectively [35,36]. For a single enzyme molecule, this is no doubt valid over the course of the experiment, even for a low substrate concentration, say in the μM range. Such considerations allow one to proceed analytically and express the single molecule data and results in compact forms [10].

With this background, here we investigate the stochastic kinetics and the thermodynamics of single molecule enzyme catalysis going beyond the chemiostatic condition. This is obtained by making the substrate concentration oscillatory, periodic to be specific. We clarify that, the single enzyme molecule 'sees' a time-varying substrate concentration $[\mathbf{S}](t)$ which is realized by some external mechanism and is *not* due to the catalysis reaction itself. This time-dependent driving keeps the system out-of-equilibrium. In the long-time limit, the properties of the system also become periodic with the same period of the driving. Interestingly, the net velocity of catalysis as well as the dissipation, characterized by the total entropy production rate (EPR) [37], show hysteresis loops as a function of $[\mathbf{S}](t)$ in the long-time limit. The loop area is a measure of such hysteresis which is dynamic [38,39], i.e., generated in time due to the periodic driving. Recently, such kind of feature is shown to occur in ion channels for a range of frequencies of the external driving [40]. However, for such a system, in absence of time-dependent driving, equilibrium is reached. This is unlike our case where, even for fixed $[\mathbf{S}]$ (and $[\mathbf{P}]$) representing constant driving, the system attains NESS. In this work, we also get a similar aspect of vanishing hysteresis in the low and high-frequency limits of substrate oscillation; this is found to be true both for velocity and dissipation. The interplay between the time-scales of system's intrinsic

relaxation and external driving begs for a deeper understanding of the mechanism behind dissipation. To this end, we analyze the recently introduced concepts of adiabatic and nonadiabatic contributions to the total EPR [41]. They are also found to exhibit similar hysteresis loops against $[\mathbf{S}](t)$ along with the vanishing loop area in the limiting conditions. However, the average, over a period, of all the quantities in the long-time limit increase to saturation with rising frequency of substrate oscillation. We also discuss about a feasible experimental protocol to realize such dynamic hysteresis features.

2 Single enzyme catalysis with oscillatory substrate input

We consider here the catalytic reaction of a single enzyme molecule having a single substrate binding site. At any instant of time, the enzyme can be in the free (unbound) state, E or in the substrate-bound state, ES with some probability. The reaction scheme is written following the MM kinetics

$$\mathrm{E} + \mathrm{S} \underset{\mathrm{k}_{-1}}{\overset{\mathrm{k}_1'}{\rightleftharpoons}} \mathrm{ES} \underset{\mathrm{k}_2'}{\overset{\mathrm{k}_{-2}}{\rightleftharpoons}} \mathrm{E} + \mathbf{P}$$

where the rate constant $k_2^{'}$ is introduced only to avoid the divergence of total EPR (and not from any kinetic mechanistic viewpoint). The value of $k_2^{'}$ is taken to be very small (but greater than zero). Hence, its contribution to the reaction kinetics as well as thermodynamics is negligible.

The kinetics can be further simplified by taking the substrate and product concentrations as fixed. This is the well-known chemiostatic condition with suitably chosen influx and efflux of **S** and **P**, respectively, that leads the reaction system to a NESS instead of equilibrium. The above reaction scheme then reduces to

$$\mathrm{E} \underset{\mathrm{K}_2}{\overset{\mathrm{K}_1}{\rightleftharpoons}} \mathrm{ES}. \tag{1}$$

Here, $K_1 = (k_1^{'}[\mathbf{S}] + k_2^{'}[\mathbf{P}]) = (k_1 + k_2)$ is the total formation rate constant of ES and $K_2 = (k_{-1} + k_{-2})$ is its total dissociation rate constant. It is to be noted that, in a closed system, the depletion of substrate concentration from its initial value, even say in μM range, by a single enzyme molecule is only slight and results in the pseudo-first order kinetics. However, the latter case is thermodynamically distinct although kinetics is identical.

Now, we consider the substrate concentration to be oscillatory: $[\mathbf{S}](t) = [\mathbf{S}]_0 + [\mathbf{S}]_a \sin^2 2\pi\nu t$ with effective frequency $4\pi\nu$. This may be experimentally realized with stepwise injection of substrate at a periodically varying rate which can create an environment of oscillatory substrate concentration around the single enzyme molecule. Increase in the number of such of steps should better match the continuous case, as will be shown letter. The effective first-order rate constant gets modified as $k_1(t) = k_1^{'}[\mathbf{S}](t)$. The stochastic enzyme kinetics is described in terms of the following CME

$$\frac{\partial P(n,t)}{\partial t} = \sum_{\mu=\pm1}^{\pm2} \left[w_\mu(n-\boldsymbol{\nu_\mu}, n)(t) P(n-\boldsymbol{\nu_\mu}, t) - w_{-\mu}(n, n-\boldsymbol{\nu_\mu})(t) P(n,t) \right]. \tag{2}$$

Here, $P(n,t)$ is the probability to find the enzyme in state-n (=0,1) at time t; $n = 0$ means the free enzyme state, E and $n = 1$ is the bound enzyme state, ES. The stoichiometric coefficient of the μ-th reaction is denoted by $\boldsymbol{\nu_\mu}$ and the corresponding rate constant by k_μ. $\boldsymbol{\nu_\mu} = 1$ for $\mu = 1, 2$ and $\boldsymbol{\nu_\mu} = -1$ for $\mu = -1, -2$. Then, the transition rates from state-$(n - \boldsymbol{\nu_\mu})$ to state-n become $w_\mu(0,1)(t) = k_\mu(t)$ for $\mu = 1, 2$ and $w_\mu(1,0)(t) = k_\mu(t)$ for $\mu = -1, -2$. Actually, except $w_1(0,1)(t)$, all the other transition rates are time-independent. The net velocity of catalysis is expressed in terms of the state probabilities as

$$v_{\text{net}}(t) = k_{-2} P(1,t) - k_2 P(0,t) = (k_{-2} + k_2) P(1,t) - k_2. \tag{3}$$

The solution of Eq. (2) is given by

$$P(1,t) = P(1,t_0) \exp\left[-\int_{t_0}^{t} K(t')dt' \right] + \int_{t_0}^{t} K_1(t') \exp\left[-\int_{t'}^{t} K(t'')dt'' \right] dt' \tag{4}$$

where $K(t) = K_1(t) + K_2$. Using Eq. (4), for $mT < t < (m+1)T$, $P(1,t)$ can be written as [40]

$$P(1, mT + t) = P(1, mT) \exp\left[-\int_{mT}^{t} K(t')dt' \right] + \int_{mT}^{t} K_1(t') \exp\left[-\int_{t'}^{t} K(t'')dt'' \right] dt', \tag{5}$$

where T is the time period of the oscillating substrate concentration and $m(= 0, 1, 2, \ldots.)$ is the number of such periods. From Eq. (4), a recursion relation can be constructed

$$P(1, (m+1)T) = \phi P(1, mT) + \Delta_0, \tag{6}$$

where ϕ and Δ_0 are given by

$$\phi = \exp\left[-\int_0^T K(t)dt \right] \tag{7}$$

and

$$\Delta_0 = \int_0^T K_1(t') \exp\left[-\int_{t'}^{T} K(t'')dt'' \right] dt'. \tag{8}$$

From Eq. (6), one gets

$$P(1, mT) = \phi^m P(1,0) + \frac{1-\phi^m}{1-\phi} \Delta_0, \tag{9}$$

where $P(1,0)$ is the initial probability. The asymptotic value of $P(1,mT)$ is obtained at the limit $m \to \infty$ as

$$\lim_{m\to\infty} P(1,mT) = \frac{\Delta_0}{1-\phi}. \tag{10}$$

Substituting Eq. (10) into Eq. (5), we obtain in the long-time limit (denoted by superscript 'ss')

$$P^{ss}(1,t) = \lim_{m\to\infty} P(1,mT+t) = \frac{\Delta(t)}{1-\phi}. \tag{11}$$

where

$$\Delta(t) = \int_t^{t+T} K_1(t') \exp\left[-\int_{t'}^{t+T} K(t'')dt''\right] dt'. \tag{12}$$

Now, one can proceed further with Eq. (11) and inspect the limiting conditions of low and high frequency [40].

2.1 Low-frequency limit

At very low frequency with $T \to \infty$, ϕ in Eq. (7) vanishes. Therefore, $P^{ss}(1,t)$ in Eq. (11) can be written as

$$P^{ss}(1,t) = \int_0^T K_1(t-t') \exp\left[-\int_0^{t'} K(t-t'')dt''\right] dt'. \tag{13}$$

As K_1 and K are slowly-varying functions of time, one can take the following approximations

$$K_1(t-t') \approx K_1(t) - t'\dot{K}_1(t'),\ K(t-t'') \approx K(t) - t''\dot{K}(t'')$$

and

$$\exp\left[-\int_0^{t'} K(t-t'')dt''\right] \approx \left(1+\frac{1}{2}\dot{K}(t)t'^2\right)\exp\left[-K(t)t'\right]. \tag{14}$$

Neglecting the term proportional to the product $\dot{K}_1(t)\dot{K}(t)$, we obtain

$$P^{ss}(1,t) \approx P^{\mathrm{st}}(1,[\mathbf{S}]_t) - \frac{\dot{P}^{\mathrm{st}}(1,[\mathbf{S}]_t)}{K(t)}, \tag{15}$$

where $P^{\mathrm{st}}(1,[\mathbf{S}]_t) = \frac{K_1([\mathbf{S}]_t)}{K([\mathbf{S}]_t)}$, corresponds to the steady state the system would reach if the substrate concentration were frozen at time t, at the value $[\mathbf{S}]_t$. For very slow variation of $[\mathbf{S}](t)$, the system can always follow the change without lagging. One can then safely neglect the second term in the r.h.s. of Eq. (15) leading to

$$P^{ss}(1,t) = P^{\mathrm{st}}(1,[\mathbf{S}]_t), \quad \nu \to 0. \tag{16}$$

Actually, we will get the same steady state solution as in Eq. (16) starting with constant substrate concentration value $[\mathbf{S}]_t$ [16]. The superscript 'st' in $P^{\mathrm{st}}(1,[\mathbf{S}]_t)$ denotes this fact and distinguishes the situation from the general time-dependent substrate concentration case (with superscript 'ss').

2.2 High-frequency limit

In the high frequency limit with $T \to 0$, ϕ in Eq. (7) can be written as

$$\phi = 1 - T\langle K(t)\rangle. \tag{17}$$

Here $\langle(...)\rangle = \frac{1}{T}\int_0^T (...)dt$ denotes average over a period. Then, $P^{ss}(1,t)$ in Eq. (11) takes the form

$$P^{ss}(1,t) = \frac{1}{T\langle K(t)\rangle}\int_t^{t+T} K_1\left(t^{'}\right)\exp\left[-\int_{t'}^{t+T} K\left(t^{''}\right)dt^{''}\right]dt^{'}. \tag{18}$$

Taking the following approximation

$$\exp\left[-\int_{t'}^{t+T} K\left(t^{''}\right)dt^{''}\right] \approx 1 - \int_{t'}^{t+T} K\left(t^{''}\right)dt^{''}, \tag{19}$$

Eq. (18) can be written as

$$P^{ss}(1,t) = \frac{\langle K_1(t)\rangle}{\langle K(t)\rangle} - \frac{\xi}{\int_t^{t+T} K(t^{'})dt^{'}} \tag{20}$$

with $\xi = \int_t^{t+T} K_1(t^{'})(\int_{t'}^{t+T} K(t^{''})dt^{''})dt^{'}$. The limit $t^{'}$ varies in the range, $t \le t^{'} \le t+T$ and $t^{''}$ varies in the range, $t^{'} \le t^{''} \le t+T$. As $T \to 0$, one can approximate $(\int_{t'}^{t+T} K(t^{''})dt^{''})$ as $(T+t-t^{'})K(t')$ where $0 \le (T+t-t^{'}) \le T$. This makes $\xi \approx \mathrm{T}\int_{\mathrm{t}}^{\mathrm{t+T}} \chi(\mathrm{t}^{'})\mathrm{K}(\mathrm{t}^{'})\mathrm{dt}^{'} \to 0$ in this limit. Thus, finally we obtain

$$P^{ss}(1) = \frac{\langle K_1(t)\rangle}{\langle K(t)\rangle}, \quad \nu \to \infty. \tag{21}$$

For very fast substrate oscillation, the system completely fails to sense the variation and fills only the average effect. So at $\nu \to \infty$, $P^{ss}(1)$ becomes independent of time.

2.3 Detailed and circular balance conditions

Before going into the details of stochastic thermodynamics of the system, we point out how the (net) fluxes associated with the reaction steps are related to each other.

Under the chemiostatic condition, with [**S**] (and [**P**]) fixed, the system reaches NESS where we have

$$w_1(0,1)P^{\rm st}(0,[\mathbf{S}]_t) - w_{-1}(1,0)P^{\rm st}(1,[\mathbf{S}]_t) = w_{-2}(1,0)P^{\rm st}(1,[\mathbf{S}]_t) - w_2(0,1)P^{\rm st}(0,[\mathbf{S}]_t) \neq 0. \tag{22}$$

The equality in Eq. (22) implies the fulfillment of what is known as the circular balance (CB) condition [42] whereas, the inequality corresponds to the violation of the detailed balance (DB) condition. The latter holds at equilibrium when the inequality becomes equality. In our case, it will occur when $\frac{k_1 k_{-2}}{k_{-1} k_2} = 1$. We will subsequently show that, in presence of oscillatory substrate concentration, the CB condition gets broken too.

3 Stochastic thermodynamics of MM kinetics under periodic driving

Entropy of the reaction system can be written in terms of the state-probabilities as [41]

$$S_{\rm sys}(t) = -\sum_n P(n,t)\ln P(n,t), \tag{23}$$

where the Boltzmann constant is set at $k_B = 1$. From Eq. (2), the system EPR can be split into total and medium contributions [43]

$$\dot{S}_{\rm sys}(t) = \dot{S}_{\rm tot}(t) - \dot{S}_{\rm m}(t). \tag{24}$$

They are defined as

$$\dot{S}_{\rm tot}(t) = \frac{1}{2}\sum_{n,\mu}\left[w_\mu(n-\boldsymbol{\nu_\mu},n)P(n-\boldsymbol{\nu_\mu},t) - w_{-\mu}(n,n-\boldsymbol{\nu_\mu})P(n,t)\right] \times \ln\frac{w_\mu(n-\boldsymbol{\nu_\mu},n)P(n-\boldsymbol{\nu_\mu},t)}{w_{-\mu}(n,n-\boldsymbol{\nu_\mu})P(n,t)} \geq 0 \tag{25}$$

and

$$\dot{S}_{\rm m}(t) = \frac{1}{2}\sum_{n,\mu}\left[w_\mu(n-\boldsymbol{\nu_\mu},n)P(n-\boldsymbol{\nu_\mu},t) - w_{-\mu}(n,n-\boldsymbol{\nu_\mu})P(n,t)\right] \times \ln\frac{w_\mu(n-\boldsymbol{\nu_\mu},n)}{w_{-\mu}(n,n-\boldsymbol{\nu_\mu})}. \tag{26}$$

This is the traditional way of looking into the 2nd law in irreversible thermodynamics.

Recently, another division of the total EPR into adiabatic and nonadiabatic contributions is shown to have fundamental importance regarding fluctuation theorems [29]. This division is particularly relevant when DB is not satisfied, as in our case, even with fixed [**S**] (and [**P**]). Now, it will be interesting to study the case when the substrate

concentration also varies periodically with time. The interplay between the inherent timescale of system kinetics and the timescale of external driving also demands investigation of the adiabatic and nonadiabatic contributions to the total EPR.

Following Esposito et al. [41], the total EPR can be expressed as a sum of adiabatic and nonadiabatic parts as

$$\dot{S}_{\rm tot}(t) = \dot{S}_{\rm a}(t) + \dot{S}_{\rm na}(t) \tag{27}$$

where

$$\dot{S}_{\rm a}(t) = \frac{1}{2}\sum_{n,\mu}\left[w_\mu(n-\boldsymbol{\nu_\mu},n)P(n-\boldsymbol{\nu_\mu},t) - w_{-\mu}(n,n-\boldsymbol{\nu_\mu})P(n,t)\right] \times \ln\frac{w_\mu(n-\boldsymbol{\nu_\mu},n)P^{\rm st}(n-\boldsymbol{\nu_\mu},[\mathbf{S}]_t)}{w_{-\mu}(n,n-\boldsymbol{\nu_\mu})P^{\rm st}(n,[\mathbf{S}]_t)} \tag{28}$$

and

$$\dot{S}_{\rm na}(t) = \frac{1}{2}\sum_{n,\mu}\left[w_\mu(n-\boldsymbol{\nu_\mu},n)P(n-\boldsymbol{\nu_\mu},t) - w_{-\mu}(n,n-\boldsymbol{\nu_\mu})P(n,t)\right] \times \ln\frac{P(n-\boldsymbol{\nu_\mu},t)P^{\rm st}(n,[\mathbf{S}]_t)}{P(n,t)P^{\rm st}(n-\boldsymbol{\nu_\mu},[\mathbf{S}]_t)}. \tag{29}$$

We now study the system in the long-time limit in the two limiting conditions, $\nu \to 0$ and $\nu \to \infty$.

In the low-frequency limit, it is easy to see from Eq. (16) and Eq. (29), that $\dot{S}^{ss}_{\rm na} = 0$ and thus $\dot{S}^{ss}_{\rm a}(t) = \dot{S}^{ss}_{\rm tot}(t)$. For $\nu \to 0$, $P^{\rm st}(1,[\mathbf{S}]_t) = \frac{K_1([\mathbf{S}]_t)}{K_1([\mathbf{S}]_t)+K_2}$; then, from Eq. (28), one gets

$$\dot{S}^{ss}_{\rm a}([\mathbf{S}]_t) = \left(k_1P^{\rm st}(0,[\mathbf{S}]_t) - k_{-1}P^{\rm st}(1,[\mathbf{S}]_t)\right)\ln\frac{k_1P^{\rm st}(0,[\mathbf{S}]_t)}{k_{-1}P^{\rm st}(1,[\mathbf{S}]_t)} + \left(k_2P^{\rm st}(0,[\mathbf{S}]_t) - k_{-2}P^{\rm st}(1,[\mathbf{S}]_t)\right)\ln\frac{k_2P^{\rm st}(0,[\mathbf{S}]_t)}{k_{-2}P^{\rm st}(1,[\mathbf{S}]_t)}, \quad \text{for } \nu \to 0. \tag{30}$$

From the circular balance condition, Eq. (22), we have

$$k_1P^{\rm st}(0,[\mathbf{S}]_t) - k_{-1}P^{\rm st}(1,[\mathbf{S}]_t) = k_{-2}P^{\rm st}(1,[\mathbf{S}]_t) - k_2P^{\rm st}(0,[\mathbf{S}]_t). \tag{31}$$

Using Eq. (31) along with $P^{\rm st}(0,[\mathbf{S}]_t) = (1 - P^{\rm st}(1,[\mathbf{S}]_t))$, Eq. (30) reduces to

$$\dot{S}^{ss}_{\rm a}([\mathbf{S}]_t) = \left(\frac{k_1([\mathbf{S}]_t)k_{-2} - k_{-1}k_2}{K_1([\mathbf{S}]_t)+K_2}\right)\ln\left(\frac{k_1([\mathbf{S}]_t)k_{-2}}{k_{-1}k_2}\right) = \dot{S}^{ss}_{\rm tot}([\mathbf{S}]_t), \quad \text{for } \nu \to 0. \tag{32}$$

One can see that for $\frac{k_1([\mathbf{S}]_t)k_{-2}}{k_{-1}k_2} = 1$, which corresponds to the DB condition for the enzyme catalysis at $\nu \to 0$ [see the discussion in Sect. 2 after Eq. (22)], $\dot{S}^{ss}_{\rm tot}([\mathbf{S}]_t) = 0$

as should be the case. In all other situations, $\dot{S}^{ss}_{\rm tot}([\mathbf{S}]_t) > 0$ and the reaction system remains out-of-equilibrium.

In the high-frequency limit, the state probabilities become independent of time as given in Eq. (21). Using Eq. (21) and Eq. (28), the adiabatic EPR in the long-time limit becomes

$$\dot{S}^{ss}_{\rm a}(t) = \left[\left(\frac{k_1(t)K_2 - k_{-1}\langle K_1(t)\rangle}{\langle K_1(t)\rangle + K_2}\right)\ln\left(\frac{k_1(t)K_2}{k_{-1}K_1([\mathbf{S}]_t)}\right) + \left(\frac{k_2K_2 - k_{-2}\langle K_1(t)\rangle}{\langle K_1(t)\rangle + K_2}\right)\ln\left(\frac{k_2K_2}{k_{-2}K_1([\mathbf{S}]_t)}\right)\right], \quad \text{for } \nu \to \infty. \tag{33}$$

The corresponding nonadiabatic EPR is given by

$$\dot{S}^{ss}_{\rm na}(t) = \left(\frac{K_2(K_1(t) - \langle K_1(t)\rangle)}{\langle K_1(t)\rangle + K_2}\right)\ln\frac{K_1([\mathbf{S}]_t)}{\langle K_1(t)\rangle}, \quad \text{for } \nu \to \infty. \tag{34}$$

Then, it follows that

$$\dot{S}^{ss}_{\rm tot}(t) = \left[\left(\frac{k_1(t)K_2 - k_{-1}\langle K_1(t)\rangle}{\langle K_1(t)\rangle + K_2}\right)\ln\left(\frac{k_1(t)K_2}{k_{-1}\langle K_1(t)\rangle}\right) + \left(\frac{k_2K_2 - k_{-2}\langle K_1(t)\rangle}{\langle K_1(t)\rangle + K_2}\right)\ln\left(\frac{k_2K_2}{k_{-2}\langle K_1(t)\rangle}\right)\right], \quad \text{for } \nu \to \infty. \tag{35}$$

Before ending this section, we make an important observation regarding the CB condition in Eq. (31). If we assume that Eq. (31) still holds in the $\nu \to \infty$ limit, it leads to the relation $\frac{P^{ss}(0)}{P^{ss}(1)} = \frac{K_2}{K_1(t)}$. Now, this *can not* be true as the l.h.s. of this relation is independent of time in this limit whereas, the r.h.s. is time-dependent. So, the CB condition *must also be broken*. This gives an understanding about the role of time-dependent substrate input. As the chemiostatic condition breaks the DB, the periodic oscillation disrupts the CB. Although, we are in the $\nu \to \infty$ limit, actually CB is broken for any finite ν. When CB holds but DB is broken, as in a NESS with constant [**S**], the total (and adiabatic) EPR is positive but the nonadiabatic EPR is zero in the long-time limit. Breaking of CB due to time-dependent external driving leads to a non-zero nonadiabatic EPR, as shown in Eq. (34). In the next section, numerical analysis of the single enzyme catalysis at various intermediate substrate oscillation frequencies will make these points more clear and robust.

4 Results and discussion

The numerical analysis of Eq. (2) is performed using the Heun's algorithm (time-step 10^{-5}s) with the following parameters: $k_1^{'} = 0.15\,\mu\text{M}^{-1}\text{s}^{-1}$, $k_{-1} = 7.0\,\text{s}^{-1}$, $k_{-2} = 2.0\,\text{s}^{-1}$, $k_2 = 10^{-6}\,\text{s}^{-1}$, $[\mathbf{S}]_0 = 100\,\mu\text{M}$, $[\mathbf{S}]_a = 50\,\mu\text{M}$. We show the net velocity of product formation, as a function of time and also as a function of $[\mathbf{S}](t)$ over a period, for various oscillation frequencies in Fig. 1 in the long-time limit. Comparison of $v^{ss}_{\rm net}(t)$ dynamics at low and high frequencies (see Fig. 1a, b) indicates that as

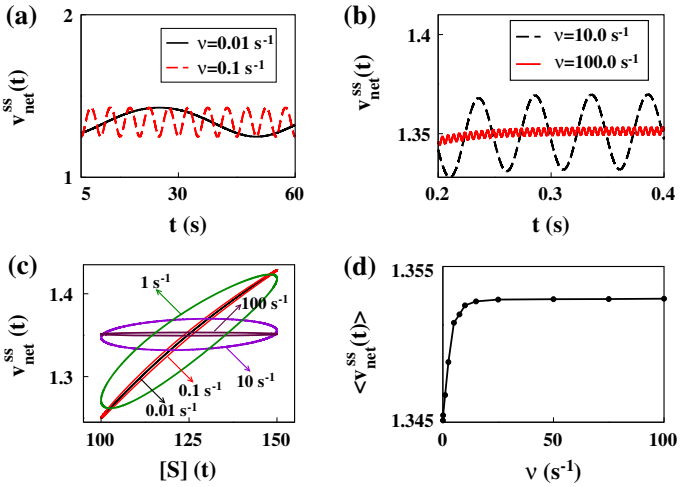

Fig. 1 **a, b** Dynamics of net velocity $v_{\text{net}}^{ss}(t)$ in the long-time limit for different substrate oscillation frequencies ν. **c** Dynamic hysteresis in the $v_{\text{net}}^{ss}(t) - [\mathbf{S}](t)$ loops generated by plotting data over a period for various ν values. **d** The average (over a period) net velocity, $\langle v_{\text{net}}^{ss}(t)\rangle$ as a function of ν

the frequency rises, the amplitude of oscillation of $v_{\text{net}}^{ss}(t)$ attenuates. This becomes particularly clear for $\nu = 10\,\text{s}^{-1}$ and $\nu = 100\,\text{s}^{-1}$, shown in Fig. 1b. This is due to the fact that at $\nu \to \infty$, the state probabilities ultimately become time-independent and this gets reflected in the dynamics of the net velocity [see Eqs. (3) and (21)]. Now, plotting $v_{\text{net}}^{ss}(t)$ as a function of $[\mathbf{S}](t)$ over a period at different frequencies generates loops of varying area as shown in Fig. 1c. At low frequencies such as $\nu = 0.01\,\text{s}^{-1}$ as well as at high frequencies such as $\nu = 100\,\text{s}^{-1}$, the loop area almost vanishes whereas at intermediate frequency values, like $\nu = 1\,\text{s}^{-1}$ and $\nu = 10\,\text{s}^{-1}$, significant loop structures are present. This phenomenon is a signature of dynamic hysteresis where the loop area of the concerned plot passes through a maximum as a function of the driving frequency. We have also shown the average (over a period) net velocity, $\langle v_{\text{net}}^{ss}(t)\rangle$ as a function of ν in Fig. 1d. $\langle v_{\text{net}}^{ss}(t)\rangle$ first rises and then saturates as ν is increased. However, as evident from Fig. 1d, the average varies little over a large range of frequency.

We find similar type of behavior for the average total EPR $\langle \dot{S}_{\text{tot}}^{ss}(t)\rangle$ as shown in Fig. 2a. It rises with ν and finally saturates, following the same trend as that of the net velocity. It also shows dynamic hysteresis as a function of $[\mathbf{S}](t)$ (see Fig. 2c); the hysteresis disappears in the limiting conditions, too. The amplitude of oscillation of $\dot{S}_{\text{tot}}^{ss}(t)$ gets reduced at higher frequencies like in the case of net velocity. Medium and system EPR also exhibit similar dynamic hysteresis behavior as shown in Fig. 2b, d, respectively. Only two curves are shown for the medium EPR for clarity. From Fig. 2d, we can see that the amplitude of oscillation of $\dot{S}^{ss}(t)$ as a function of ν follows the opposite trend compared to that of $\dot{S}_{\text{tot}}^{ss}(t)$. This is because, at low frequencies the state of the system changes very slowly; as the system entropy is a state function, so $\dot{S}^{ss}(t)$ lies close to zero. As ν increases, $\dot{S}^{ss}(t)$ starts to oscillate with higher amplitude.

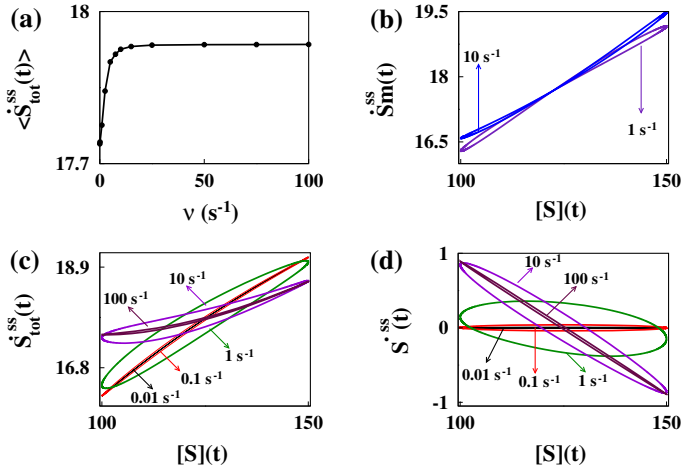

Fig. 2 **a** Plot of $\langle \dot{S}^{ss}_{tot}(t) \rangle$ as a function of ν. **b–d** Dynamic hysteresis in the loops of medium, total and system EPRs, plotted as a function of $[\mathbf{S}](t)$ for different νs

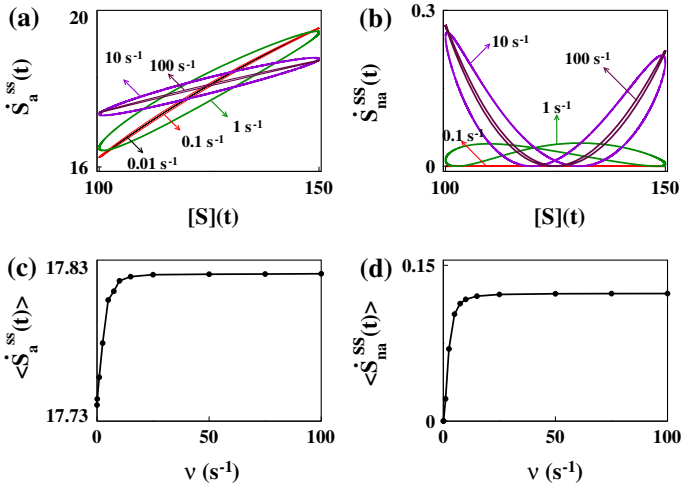

Fig. 3 **a**, **b** Dynamic hysteresis in adiabatic and nonadiabatic EPRs as a function of $[\mathbf{S}](t)$ over a period for different ν values in the long-time limit. **c**, **d** The corresponding averages as a function of ν

However, the average of $\dot{S}^{ss}(t)$ over a period is zero for any ν, again it being a state function.

Next, we have shown the corresponding plots for the adiabatic and nonadiabatic EPRs in Fig. 3. Both the quantities show dynamic hysteresis. The $\dot{S}^{ss}_{a}(t) - [\mathbf{S}](t)$ loops look quite similar to those of $\dot{S}^{ss}_{tot}(t)$ except the fact that the former is more symmetric, particularly at high frequencies (see Fig. 3a). The total EPR is thus mainly governed by the adiabatic contribution. The nonadiabatic EPR $\dot{S}^{ss}_{na}(t)$ is almost zero at low frequencies, like $\nu = 0.1\,\mathrm{s}^{-1}$ as shown in Fig. 3b. With rising ν, it develops a two-loop structure as a function of $[\mathbf{S}](t)$ and the two $[\mathbf{S}](t)$ values where $\dot{S}^{ss}_{na}(t)$

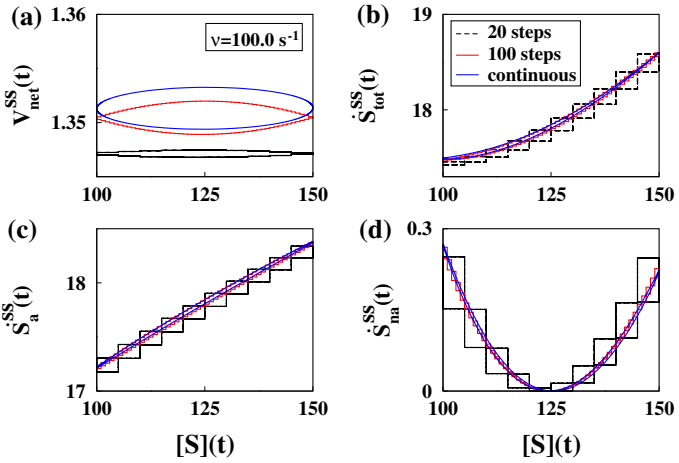

Fig. 4 The possible experimental realization of dynamic hysteresis using periodic stepwise injection of substrate. The number of such steps comprising a full oscillation cycle are taken to be 20 and 100. The theoretical results are denoted as 'continuous'. Increase in the step-number results in better reproduction of the theoretical prediction for **a** net velocity, **b** total EPR, **c** adiabatic EPR and **d** nonadiabatic EPR

becomes zero shifts in such a way that they approach each other with increasing frequency. Actually at $\nu = 100\,\mathrm{s}^{-1}$, these two points have almost merged at $[\mathbf{S}] = 125\,\mu\mathrm{M}^{-1}\mathrm{s}^{-1}$, the mean substrate concentration. We also observe that, the overall shape of the $\dot{S}^{ss}_{\mathrm{na}}(t) - [\mathbf{S}](t)$ loops are asymmetric around this point and this causes the asymmetry in the $\dot{S}^{ss}_{\mathrm{tot}}(t) - [\mathbf{S}](t)$ loops. The amplitude of oscillation of $\dot{S}^{ss}_{\mathrm{na}}(t)$ increases with ν as the driving is the source of nonadiabaticity. We have also plotted the corresponding averages in Fig. 3c, d. They also show the pattern already observed, i.e., the initial rise with frequency to a final saturation.

4.1 Practical implementation of the scheme

The effects produced due to oscillatory substrate concentration can be experimentally realized with periodic stepwise injection of substrate as already mentioned in Sect. 1. The hysteresis plots, generated at various range of frequencies, are expected to reproduce the continuous case with better accuracy as the number of such steps comprising a full cycle of concentration oscillation are increased. In Fig. 4, we show that this is indeed the case, by considering a high-frequency scenario with $\mu = 100\,\mathrm{s}^{-1}$ where theory predicts vanishing hysteresis. As the number of steps rises from 20 to 100, the discrete hysteretic responses of all the quantities are found to match the theoretically predicted continuous curves better. This can be tested, obviously most easily, by following the product formation rate in the long-time limit.

5 Conclusion

We have explored the stochastic kinetics of a single enzyme molecule following MM scheme in presence of periodic substrate input. The time-dependent driving keeps the

system in a nonequilibrium state with positive dissipation. The interaction between the system and driving time-scales is investigated in terms of the adiabatic and nonadiabatic parts of dissipation, i.e., the total EPR. Unlike in a NESS with broken DB, which is realized for constant [**S**] and [**P**], the periodic [**S**](t) also breaks the CB condition in the long-time limit. The violation of CB results in a positive nonadiabatic EPR. This is equivalent to the breaking of DB in NESS that produces positive total EPR, coming entirely from the adiabatic contribution.

Interestingly, oscillatory substrate concentration generates dynamic hysteresis not only in the net velocity of catalysis but also in the associated dissipation. Various parts of the total EPR, viz., the system, medium, adiabatic and nonadiabatic EPR individually exhibit such a feature in the intermediate frequency range. In the low and high-frequency limits, the hysteresis in all these quantities are found to disappear. However, their averages (over a period) in the long-time limit are found to rise with frequency to saturation (except system EPR whose average over a period is zero). In case of net velocity, this is analogous to the traditional hyperbolic curve as a function of [**S**]. Finally, we propose an experimental scheme to verify these theoretical features with periodic stepwise addition of substrate at different rates.

Acknowledgments K.B. acknowledges the University Grants Commission (UGC), India for Dr. D. S. Kothari Fellowship and Prof. K. Bhattacharyya for useful discussions.

References

1. H.P. Lu, L. Xun, X.S. Xie, Science **282**, 1877 (1998)
2. H. Wang, G. Oster, Nature **396**, 279 (1998)
3. G. Hummer, A. Szabo, Proc. Natl. Acad. Sci. USA **98**, 3658 (2001)
4. F. Ritort, C. Bustamante, I. Tinoco Jr, Proc. Natl. Acad. Sci. USA **99**, 13544 (2002)
5. D. Collin, F. Ritort, C. Jarzynski, S.B. Smith, I. Tinoco Jr, C. Bustamante, Nature **437**, 231 (2005)
6. F. Ritort, Adv. Chem. Phys. **137**, 31 (2008)
7. C. Jarzynski, Nat. Phys. **7**, 591 (2011)
8. T. Xia, N. Li, X. Fang, Annu. Rev. Phys. Chem. **64**, 459 (2013)
9. H. Qian, E.L. Elson, Biophys. Chem. **101–102**, 565 (2002)
10. S.C. Kou, B.J. Cherayil, W. Min, B.P. English, X.S. Xie, J. Phys. Chem. B **109**, 19068 (2005)
11. R. Grima, J. Chem. Phys. **133**, 035101 (2010)
12. A.F. Bartholomay, Biochemistry **1**, 223 (1962)
13. D.A. McQuarrie, J. Chem. Phys. **38**, 433 (1963)
14. D.A. McQuarrie, C.J. Jachimowski, M.E. Russell, J. Chem. Phys. **40**, 2914 (1964)
15. D.T. Gillespie, Phys. A **188**, 404 (1992)
16. B. Das, G. Gangopadhyay, J. Chem. Phys. **132**, 135102 (2010)
17. T.G. Kurtz, J. Chem. Phys. **57**, 2976 (1972)
18. P. Aranyi, J. Toth, Acta Biochim. Biophys. Acad. Sci. Hung. **12**, 375 (1977)
19. H. Qian, Annu. Rev. Phys. Chem. **58**, 113 (2007)
20. R. Grima, J. Chem. Phys. **132**, 185102 (2010)
21. A. Cornish-Bowden, *Fundamentals of Enzyme Kinetics* (Portland Press, London, 2004)
22. K. A. Johnson, R. S. Goody, Biochem. **50**, 8264 (2011) (Translation of the 1913 Michaelis–Menten Paper)
23. B.P. English, W. Min, A.M. van Oijen, K.T. Lee, G. Luo, H. Sun, B.J. Cherayil, S.C. Kou, X.S. Xie, Nat. Chem. Biol. **2**, 87 (2006)
24. C.Y. Mou, J.-L. Luo, G. Nicolis, J. Chem. Phys. **84**, 7011 (1986)
25. K.L.C. Hunt, P.M. Hunt, J. Ross, Phys. A **147**, 48 (1987)
26. P. Gaspard, J. Chem. Phys. **120**, 8898 (2004)

27. T. Schmiedl, U. Seifert, J. Chem. Phys. **126**, 044101 (2007)
28. J. Schnakenberg, Rev. Mod. Phys. **48**, 571 (1976)
29. M. Esposito, C. Van den Broeck, Phys. Rev. Lett. **104**, 090601 (2010)
30. H. Ge, H. Qian, Phys. Rev. E **81**, 051133 (2010)
31. K. Banerjee, J. Math. Chem. **52**, 2259 (2014)
32. R.K.P. Zia, B. Schmittmann, J. Phys. A **39**, 407 (2006)
33. H. Ge, M. Qian, H. Qian, Phys. Rep. **510**, 87 (2012)
34. L. Jiu-li, C. Van den Broeck, G. Nicolis, Z. Phys. B **56**, 165 (1984)
35. W. Min, L. Jiang, J. Yu, S.C. Kou, H. Qian, X.S. Xie, Nano Lett. **5**, 2373 (2005)
36. K. Banerjee, K. Bhattacharyya, Chem. Phys. **438**, 1 (2014)
37. S.R. de Groot, P. Mazur, *Non-equilibrium Thermodynamics* (North-Holland, Amsterdam, 1962)
38. B.K. Chakrabarty, M. Acharyya, Rev. Mod. Phys. **71**, 847 (1999)
39. M. Das, D. Mondal, D.S. Ray, J. Chem. Phys. **136**, 114104 (2012)
40. M.A. Pustovoit, A.M. Berezhkovskii, S.M. Bezrukov, J. Chem. Phys. **125**, 194907 (2006)
41. M. Esposito, C. Van den Broeck, Phys. Rev. E **82**, 011143 (2010)
42. H. Ge, M. Qian, H. Qian, Phys. Rep. **510**, 87 (2012)
43. D. Kondepudi, I. Prigogine, *Modern Thermodynamics (from Engines to Dissipative Structures)* (Wiley, New York, 2002)